JOURNAL OF MATERIALS SCIENCE 32 (1997) 475–482

Mechanical characterization by dynamical tensile loading of 2017 aluminium alloy joints welded by diffusion bonding. New results and SEM observations of the failure surfaces

O. DEBBOUZ*, F. NAVAÏ
Laboratoire de Sciences des Surfaces et Interfaces en Mécanique, ISITEM, Université de Nantes, La Chantrerie CP 3023, 44087 Nantes Cedex 03, France

Earlier dynamical tensile loading measurements, performed with the help of a Hopkinson bar assembly line, on diffusion-welded joints of 2017 aluminium–copper alloys, have been completed. The welding temperature was changed from 500 °C to 575 °C, the welding time was fixed at either 30 min or 2 h, and the welding pressure at either 2 or 5 MPa. Measurements of the mechanical properties were also performed on treated specimens which were base-material specimens subjected to the same thermal cycle as the welded samples. These results, obtained up to 600 °C, have been used as a reference for a direct comparison with the welded sample strengths. The more precise measurements reported here agree well with the earlier results. However, they reveal, at high temperatures (above 575 °C), a large decrease in the tensile strength of the treated specimens, which was not observed previously. Moreover, they allow the effects of the welding pressure and time on the welded joint strength to be distinguished more precisely. In order to gain a better understanding of the relationship between the welded joints dynamical properties and their microstructures, the failure surfaces were observed by scanning electron microscopy. In addition, some energy-dispersive X-ray spectra were also recorded in order to reveal the chemical nature of the failure surfaces. At low temperatures, the failure surface of the welded specimens was smooth and precipitate-free. On the contrary, at high temperatures, the failure surface was characteristic of a ductile failure mode and exhibited two kinds of precipitates, one rounded and the other oblong, at the origin of dimple formation.

1. Introduction

To avoid metal fusion problems (granular growth, cracks, residual thermal tensions …), it is rather better to use the diffusion welding process. This solid-state joining technique is a priori well adapted for welding materials exhibiting a high solidification crack susceptibility [1–3]. The age-hardenable aluminium–copper alloy 2017, which is increasingly employed in the aerospace industry [4] is a good example of this kind of material. Diffusion welding also allows the realization of pieces net to dimensions, making the process less material-consuming than machining.

Despite successful industrial applications of the diffusion welding process, the industrial non-destructive evaluation of diffusion welded joints is still difficult [4]. Thus, it is necessary to determine, very precisely in the laboratory, the best working conditions required to obtain the highest mechanical properties of the welded joints. This is a very long task because of the great number of process parameters.

The influence of the main diffusion welding parameters (temperature, time, pressure, atmosphere and surface preparation) on the mechanical properties of A 2017 alloy welded joints was studied under dynamic loading [1]. This study has shown at temperatures lower than 525 °C and for reasonably short welding times (30 min or 2 h), small welded joints strength in comparison to the that of the base material. On the contrary, above 525 °C, tensile strengths close to that of the base material could be reached, though the elongation at failure of the welded samples remained very weak and rupture occurred in the initial interface [1].

Observations by scanning electron microscopy (SEM), carried out to investigate more closely the fractured surfaces of the welded joints subjected to dynamic tensile loading at lower welding temperatures, showed failure surfaces with a brittle fracture and a smooth aspect. However, at welding temperatures higher than 550 °C the failure surface exhibited

* Author to whom all correspondence should be addressed.

0022–2461

many dimples characterizing a ductile fracture. It was found that the difference in the brittle (at lower welding temperatures) or ductile (at higher welding temperatures) nature of the welded sample failure should be more obvious by analysing the failure surface chemical composition by X-ray spectroscopy. Thus, with the aim of completing the earlier mechanical characterization of the A 2017 diffusion welded joints, some new dynamic tensile loading tests were carried out.

2. Experimental procedure

2.1. Base material and welding process

The base material was the commercial aluminium–copper alloy A2017 (supplied in the T4 metallurgical state), the chemical composition of which is given in Table I.

After machining of the two pieces to be welded, the faying surfaces were submitted to the same initial preparation which consisted of a mechanical polishing with emery paper (grades 600 and 1200). Then, the pieces were cleaned in an ultrasonic bath of acetone and finally dried in a hot air flow. Immediately after this surface preparation, the pieces were placed in the welding apparatus so that the polished grooves of the two faying surfaces were in crossed positions.

The diffusion welding was carried out at a pressure of about 10^{-5} Pa using the experimental set-up reported in previous papers [2, 3]. External pressure was applied on the pieces only when the welding temperature was reached, and it was maintained at a constant value throughout the welding process and during the major part of the cooling step.

2.2. Sample preparation

All the new tested samples were welded by using the same general procedure as described previously [1]. The welding temperature was changed from 500–575 °C and for each temperature, three samples were welded, two with a welding pressure of 2 MPa and one with 5 MPa. In the former case, the welding time was fixed at either 30 min or 2 h, whereas in the latter case the welding time was 30 min. Hence, it is expected that the new results could help to determine definitely the best choice of the welding parameters leading to the highest welded joint mechanical properties. After welding, the samples were machined in order to present, in their central part, a cylindrical shape of 5 mm diameter and 30 mm length (Fig. 1). The two extremities of the specimen were threaded so as to fix it on the two Hopkinson bars of the test apparatus as described previously [1].

2.3. Dynamic tensile loading test

All the present tests and measurements were performed with the dynamic linear assembly device and under the same experimental parameters already used in the first study [1]. More precisely, the projectile mass and length ($m = 308$ g, $l = 200$ mm), projectile moving velocity ($v = 30\ \mathrm{m\,s^{-1}}$) and the Hopkinson bars length, were kept unchanged so that the earlier experimental conditions could be well reproduced. The load exerted on the sample was evaluated by measuring the tensile stress wave, $\sigma_1(t)$, transmitted by the sample to the entrance bar. The incident stress wave generated by the impact of the projectile on the entrance bar and the reflected stress wave, $\sigma_2(t)$, at the left-hand end of the exit bar are of the same magnitude and the strain rate value is constant ($\dot{\varepsilon} = 950\ \mathrm{s^{-1}}$). From a knowledge of the reflected stress wave, $\sigma_2(t)$, and the transmitted stress wave, $\sigma_1(t)$, it is possible to calculate the stress exerted at time, t, on the sample as follows

$$\sigma(t) = \frac{\sigma_1(t)S[1-\varepsilon(t)]}{S_0} \quad (1)$$

and the strain from

$$\varepsilon(t) = \frac{c}{EL_0}\int_0^t [\sigma_2(t)-\sigma_1(t)]\,\mathrm{d}(t) \quad (2)$$

where c is the wave velocity in the Hopkinson bars ($c = (\sqrt{E/\rho})^{1/2} = 4930\ \mathrm{m\,s^{-1}}$), E and S are the Young's modulus and the cross-section of these bars, respectively ($E = 1.89 \times 10^{11}$ Pa), L_0 the initial length of the loaded sample and S_0 its initial cross-section. From a knowledge of the exerted stress and the strain elongation at time t, it is also possible to calculate the welded sample failure energy, W, per unit volume, from

$$W(t) = \int_0^{\varepsilon_r} \sigma(t)\,\mathrm{d}\varepsilon(t) \quad (3)$$

Moreover, this parameter also characterizes the welded joint toughness which represents the total area under the stress–elongation curve, up to the tensile strain failure, ε_r. To make sure that either the welded sample or the treated base material failure was evident under the tensile stress wave effect, the time duration of the transmitted wave was kept shorter than that of the reflected wave ($t = 114$ μs).

TABLE I Chemical composition of the base material (wt %)

	Si	Fe	Cu	Mn	Mg	Cr	Zn	Ti + Zr	Al
Min.	0.2		3.5	0.4	0.4				Balance
Max.	0.8	0.7	4.5	1.0	1.0	0.1	0.25	0.25	Balance

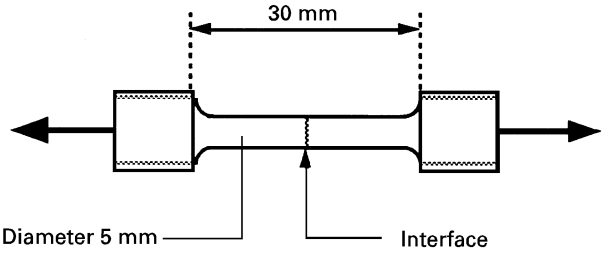

Figure 1 Shape of the dynamical tensile-tested samples.

3. Results

3.1. Dynamic stress–elongation behaviour law

In this paper, we report first the dynamic mechanical properties of two different commercial rods of A2017 as they were supplied in the T4 state. The results in Fig. 2, showed that the tensile strengths reached values between 440 and 520 MPa, with total elongations ranging from 15–18%. One can notice clearly the spread of the measurements on the base material tensile strength and elongation, which is related to the rods of different origin and their minor compositional variations. It is expected that after the thermal treatment cycle, these spreads will be subsequently reduced. The stress–elongation curves of either rod 1 or 2 (Fig. 2) present a large number of fluctuations followed, at first, by a sharp peak related to the taking up of play between the loaded sample and the Hopkinson bars. These fluctuations are interpreted as artefacts arising from reflections of the stress wave from the threaded parts of the loaded sample.

However, these results cannot be used as a reference for a direct comparison with the welded sample strengths. Indeed, the mechanical properties of the two welded pieces are more or less strongly modified by the thermal treatment imposed during the welding procedure. Therefore, for a realistic comparison, it is necessary to measure the dynamic mechanical properties of the base material after the thermal cycle. For this base material samples were heated to the welding temperatures, maintained for 30 min or 2 h and then cooled under the same conditions as the welded samples. These samples will be called "treated samples", here.

The dynamic mechanical properties of the samples thermally treated at 500 °C for 30 min are shown in Fig. 3 (curve a), where they are compared with those treated at 500 °C for 2 h (curve b). As can be seen, the dynamic behaviour of the two samples is similar, up to the failure elongation. In this case, the strength and the failure elongation values are, respectively, of the same magnitude of about 350 MPa and 18%. In fact, the failure elongation is higher than 18% except for those samples heated at 575 and 600 °C, whatever the welding time (Fig. 4). For a heating temperature of 575 °C (Fig. 4a), the strength of the treated samples for 30 min or 2 h is of the same magnitude as 390 MPa, whereas the failure strain values are, respectively, about 14% and 17%. In contrast, for a heating temperature of 600 °C (Fig. 4b), the mechanical properties of the base material are strongly damaged either for 30 min or 2 h.

In spite of the large number of fluctuations on the stress–elongation curves, it was possible, during the tensile loading measurements, to evaluate the failure

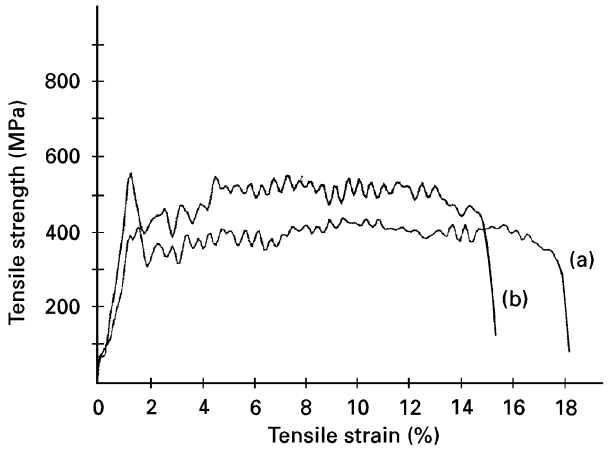

Figure 2 Dynamic stress–elongation behaviour laws for the base metal supplied in the T4 metallurgical state. (a) Rod 1, (b) rod 2.

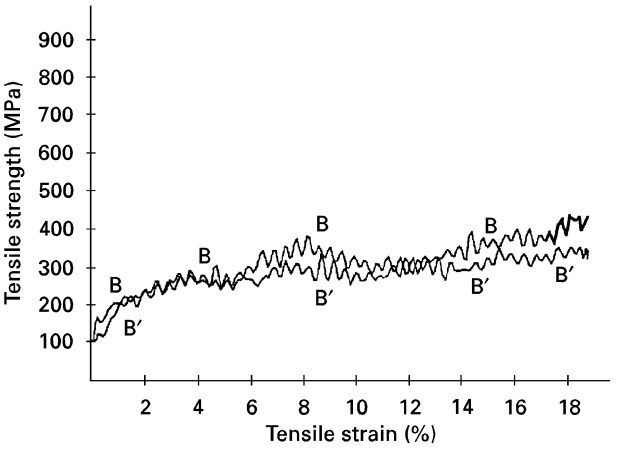

Figure 3 Dynamic stress–elongation behaviour laws for treated samples heated at 500 °C for (B) 30 min and (B′) 2 h.

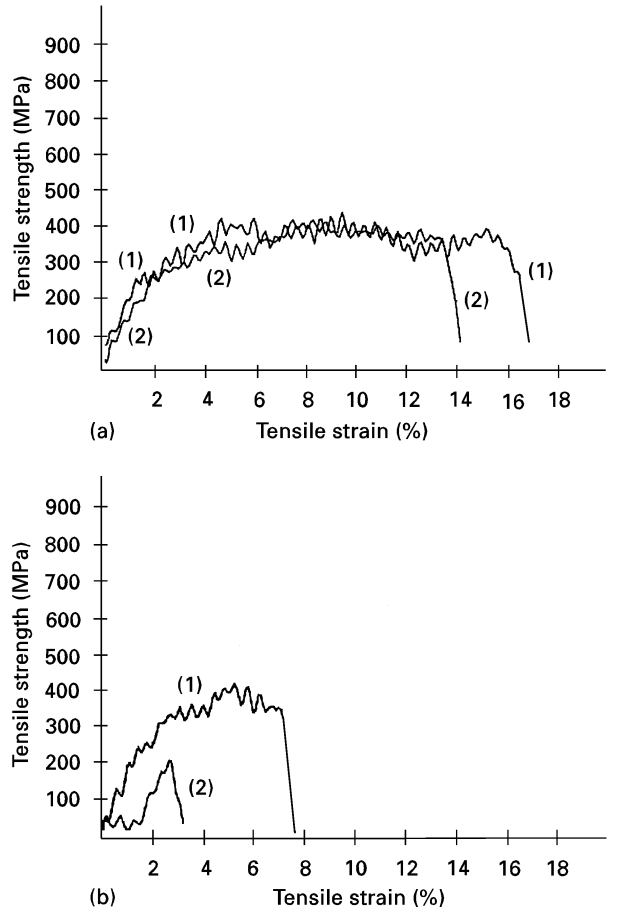

Figure 4 Dynamic stress–elongation behaviour laws for treated samples heated for (1) 30 min and (2) 2 h at different temperatures of (a) 575 °C and (b) 600 °C.

energy needed to break either the welded or the treated samples by integrating Equation 3, up to failure elongation. From the results shown in Fig. 3, the failure energy of the samples treated at 500 °C, for 30 min or 2 h is respectively, 44 and 48 J. A subsequent increase of the heating temperature from 500 °C to 550 °C, either for 30 min or 2 h (Figs 5 and 6), increases the failure energy, respectively, to 45 and 62 J, which are the maximum values reached by the treated samples (see also Fig. 9).

The dynamic mechanical properties of the samples thermally treated at 550 °C, for 30 min are exhibited in Fig. 5 (curve a), where they are compared to those of a sample welded for 30 min at 550 °C, under a welding pressure of 2 MPa (curve b). As can be seen, at lower values of elongation (less than 2%), the dynamic behaviour of the two samples is almost similar, whereas above this value, the strength failure values are slightly different. The main difference arises from the fact that the welded sample fails for an elongation of less than 11%, while the failure elongation of the treated sample is more than 18%, i.e. nearly twice that of the welded sample. Consequently, the strength of the treated base material is about 36 MPa compared to 270 MPa for the welded sample, that is about 75% of the treated base material strength.

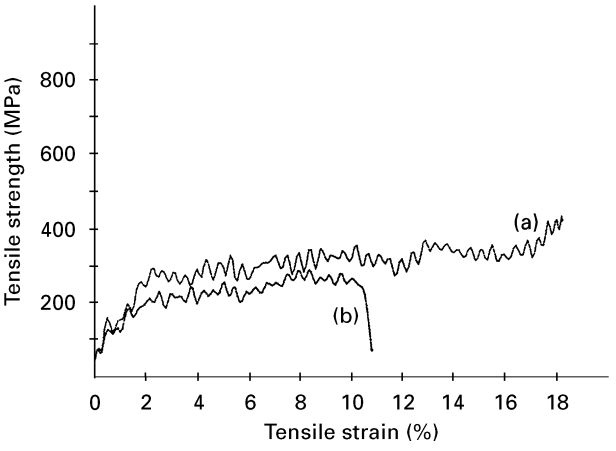

Figure 5 Dynamic stress–elongation behaviour laws for (a) treated samples heated for 30 min at 550 °C and (b) samples welded for 30 min at 550 °C and 2 MPa.

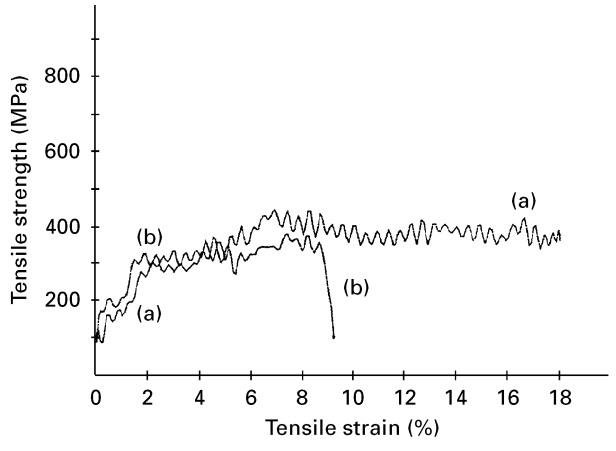

Figure 6 Dynamic stress–elongation behaviour laws for (a) treated samples heated for 2 h at 550 °C and (b) for samples welded for 2 h at 550 °C and 2 MPa.

For a fixed welding pressure of 2 MPa and for 550 °C, an increase in the welding time from 30 min to 2 h enhances significantly the welded joint tensile strength. Thus, from Fig. 6, the dynamic behaviour law of the two samples is seen to be almost identical at lower values of elongation. The difference arises from the fact that the welded sample fails for an elongation of about 9%, whereas the failure elongation of the treated sample is at least 18%, i.e. twice that of the welded sample. Consequently, the strength of the treated sample reaches 400 MPa whereas that of the welded sample is limited to 370 MPa.

3.2. Influence of the welding parameters

The tensile strength, failure elongation and failure energy of the welded samples were investigated as a function of the welding temperature, for the three sets of welding pressure and welding time described in Section 2.2. With the aim of comparison, the above mechanical properties were also measured on the treated samples heated to the welding temperature for 30 min or 2 h.

To reduce the experimental uncertainty, which was very large in the previous study [1], three tests for each set of welding parameters were carried out. The mean value for each measured mechanical property was deduced then reported on the same curve. Similar considerations apply to the tensile strain and failure energy values of both the treated and the welded samples. To facilitate the comparison, all the tensile strengths of the treated samples for 30 min or 2 h, have been reported on the same figure. Fig. 7 shows the new dynamic experimental results obtained for the three diffusion welding sets (30 min, 2 MPa; 30 min, 5 MPa; 2 h, 2 MPa).

The tensile strength curves of the samples thermally treated for 30 min or 2 h (curves 1 and 2) show two different domains. First, the failure strength follows approximately a (different) linear relationship, up to 550 °C. Above this temperature, the strength decreases

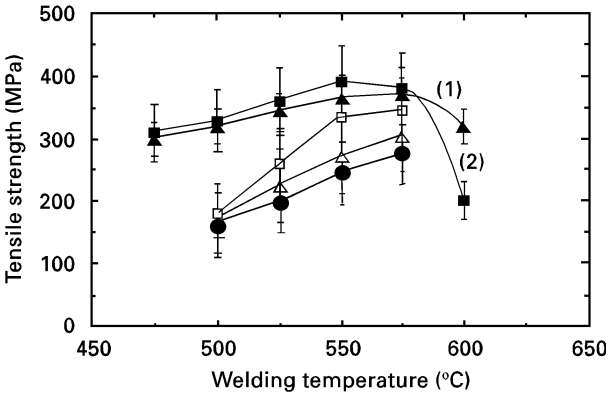

Figure 7 Results obtained for the strength as a function of the welding temperature for three different sets of operating parameter values and for base material submitted to the same thermal cycle. (▲) Base metal (30 min), (■) base metal (2 h), (●) welded joint (30 min, 2 MPa), (△) welded joint (30 min, 5 MPa), (□) welded joint (2 h, 2 MPa).

slowly to 310 MPa (curve 1), whereas that of the treated samples for 2 h (curve 2) is limited to 200 MPa at 600 °C. Hence, this temperature must be avoided because of the strong damage caused to the mechanical properties of the base metal. On the other hand, below the welding temperature of 500 °C, the dynamic strength of the welded samples remains very weak, because of the welded joint embrittlement, during their fixing on the two Hopkinson bars.

The strength of the welded samples remains substantially lower than that of the treated samples, as long as the welding temperature is below 525 °C. Above this temperature, the spread on the tensile strength results is reduced and the joint strength is of the same magnitude as that of the treated samples. For a welding pressure of 2 MPa the increasing rate of dynamic strength as a function of the welding temperature is clearly higher for a welding time of 2 h than for 30 min, and the increase in the strength values is visible above 500 °C. Such an increase was not observed under static loading tests [2, 3].

An increase in the welding pressure from 2 MPa to 5 MPa enhances significantly the strength of the welded joint for 30 min (Fig. 7). In this case, the increasing rate of the failure strength follows a linear relationship in the welding temperature range of 500–575 °C. This was clearly established in static loading [2, 3] but not in the first dynamic loading tests [1]. In the latter case, the welded samples strength was supposed to be unchanged within experimental uncertainty, because of the small number of samples tested. However, the increase in the welding pressure from 2 MPa to 5 MPa leads to an important increase of welding deformations and even to the crushing of the welded samples for 2 h at 575 °C. Therefore, the welding parameter set of (2 h, 5 MPa) was not performed in this study. It can thus be considered that any increase in the welding pressure, at least above 2 MPa, has to be avoided.

Fig. 8 shows similar results for the failure elongation. It is observed that for the treated samples either for 30 min or 2 h, the failure strain is nearly independent of the heating temperature, respectively, at about 16% and 18%, up to 550 °C. Above this temperature, the failure strain decreases slowly then rapidly down to 6%, at 600 °C (curve 2). Here, in contrast to the tensile strength, the strain values of the welded samples remain clearly smaller than those of the treated samples, whatever the welding temperature, except at 575 °C. In fact, at this temperature, the difference between the base material tensile strain and that of the welded samples becomes very small. In this case, the strain of the welded sample is about 11% for 2 h, whereas that of the treated sample, is about 15%. For a welding pressure of 2 MPa, the increasing rate of the failure strain as a function of the welding temperature is clearly higher for a welding time of 2 h than 30 min. Thus, the influence of the welding parameters on the welded joint mechanical properties seems to be significant, as a consequence of the reduction in spread of the measurements.

The failure energy results are shown in the Fig. 9. It can be noticed that the failure energy of the treated samples for 30 min, in the studied temperature range, is nearly constant at about 45 J up to 575 °C (curve 1). Above this temperature, the failure energy decreases slowly down to 35 J. In contrast, for a heating time of 2 h (curve 2), the failure energy depends on the heating temperatures, as a consequence of the strong modifications occurring in the base material structures. It is also observed that even with the reduction of experimental uncertainties, the failure energy of the welded joints always remains lower than that of the treated samples, whatever the welding parameters. Thus, for a welding temperature of 500 °C, the failure energy does not exceed 10 J, whereas that of the treated sample is larger than 40 J, i.e. nearly four times that of the welded sample.

For a fixed welding time of 30 min, the failure energy (curves 3 and 4) remains substantially low and practically unchanged by an increase in the welding pressure from 2 MPa to 5 MPa. In this case, the failure energy seems to be independent of the welding pressure and follows approximately a linear

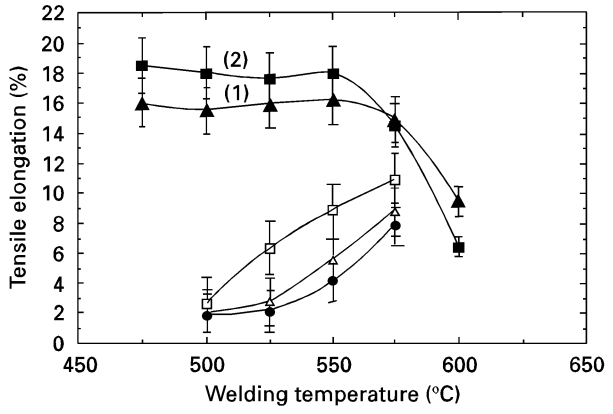

Figure 8 Results of the failure strain as a function of the welding temperature for three different sets of operating parameter values and for base material submitted to the same thermal cycle. (▲) Base metal (30 min), (■) base metal (2 h), (●) welded joint (30 min, 2 MPa), (△) welded joint (30 min, 5 MPa), (□) welded joint (2 h, 2 MPa).

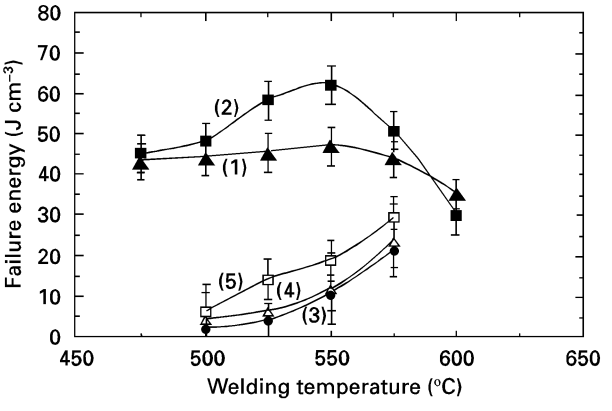

Figure 9 Results obtained for the failure energy as a function of the welding temperature for three different sets of the operating parameters and for base metal submitted to the same thermal cycle. (▲) Base metal (30 min), (■) base metal (2 h), (●) welded joint (30 min, 2 MPa), (△) welded joint (30 min, 5 MPa), (□) welded joint (2 h, 2 MPa).

relationship with the welding temperature above 525 °C. Below this temperature, the failure energy is rather constant and does not exceed the value of 6 J. In contrast, for a welding time of 2 h the failure energy follows a nearly linear relationship with the welding temperature (curve 5). Such observations were not clearly established in the previous study [1].

3.3. SEM observations and X-ray analysis

In order to understand better both the dynamic mechanical properties of the welded joints and the phenomena arising during the welding operation, some SEM observations were performed on the fractured surfaces of the tested samples. Typical fractured surfaces of dynamic loading specimens are exhibited in Fig. 10. They were carefully examined by scanning electron microscopy. For a welding temperature of 500 °C and a welding time of 30 min (Fig. 10a), the failure surface clearly shows the residual mechanical polishing features and some obvious brittle patches, suggesting that the mechanical properties of the welded joints are very weak.

An increase in the welding temperature from 500 °C to 575 °C (Fig. 10b) changes the failure morphology from a brittle aspect to ductile failure, in the presence of some dimples. In this case, the mechanical polishing grooves have completely disappeared and some fine ductile dimples are observed, where parent metal has been pulled out. This suggests that the failure occurred in the base-material mass, in the presence of some apparent yielding of the failure surface. This is due to the enhanced diffusional process coupled with higher liquid volume fractions present in the welded joint. Such a morphology difference probably explains the strength enhancement which is observed at high welding temperatures (see also Fig. 7).

For a welding time of 2 h, the fractured surfaces of the loaded samples are shown in Fig. 11. For a welding temperature of 500 °C (Fig. 11a), the fractured surface consisted of some pulled out brittle patches showing the coexistence of welded and adhesive zones, suggesting that the failure occurred in the initial interface. Some partially welded zones of different shapes and distributions are observed as well as the mechanical polishing striations, which remain visible. In this case, the diffusion process was not achieved and the joint strength is weak. The failure surface of a tested sampled welded at 575 °C (Fig. 11b) shows some dimples of a conventional ductile failure, while the polishing striations disappeared. In view of these results, it seems that the presence of precipitates, in the welded joint, enhances the strength of the tested sample.

Fig. 12 shows fractured surfaces of tested specimens welded at 500 and 575 °C for 30 min, under a welding pressure of 5 MPa. In the former case (Fig. 12a), some

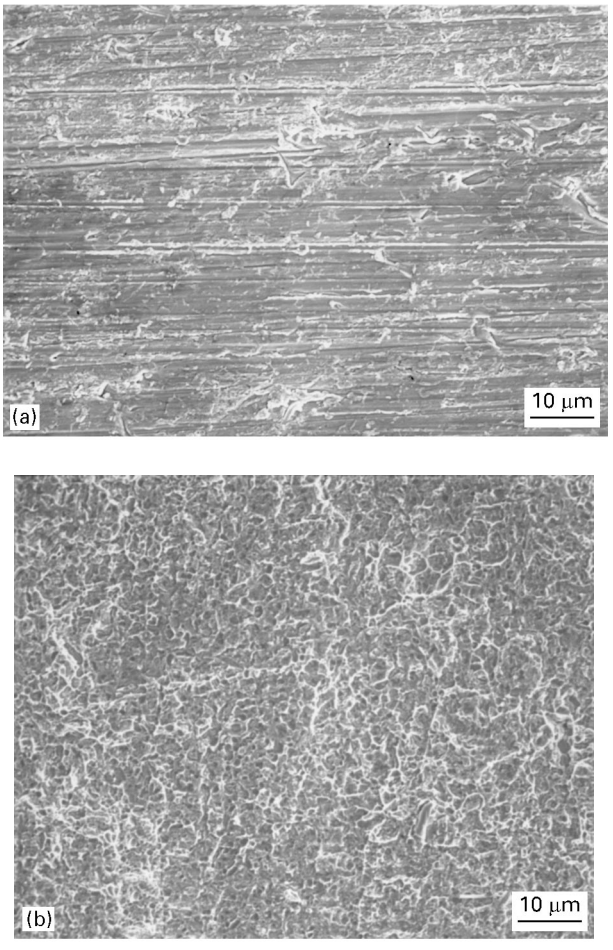

Figure 10 Scanning electron micrographs of the failure surface of welded joints after the dynamic tensile loading test. Welding temperature: (a) 500 °C and (b) 575 °C. ($P = 2$ MPa, $t = 30$ min.)

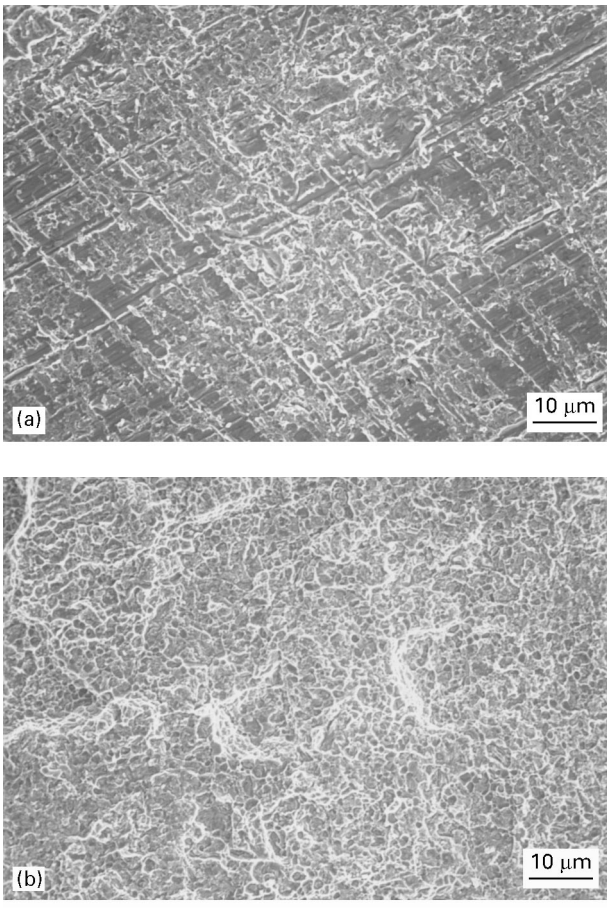

Figure 11 Scanning electron micrographs of the failure surface of welded joints after the dynamic tensile loading test. Welding temperature: (a) 500 °C and (b) 575 °C. ($P = 2$ MPa, $t = 2$ h.)

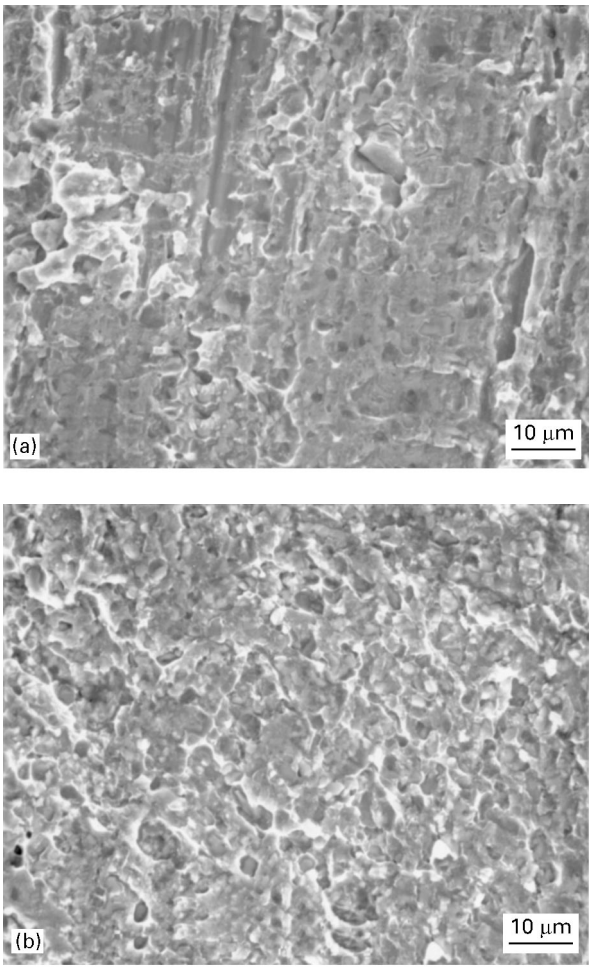

Figure 12 Scanning electron micrographs of the failure surface of welded joints after the dynamic tensile loading test. Welding temperature: (a) 500 °C and (b) 575 °C. ($P = 5$ MPa, $t = 30$ min.)

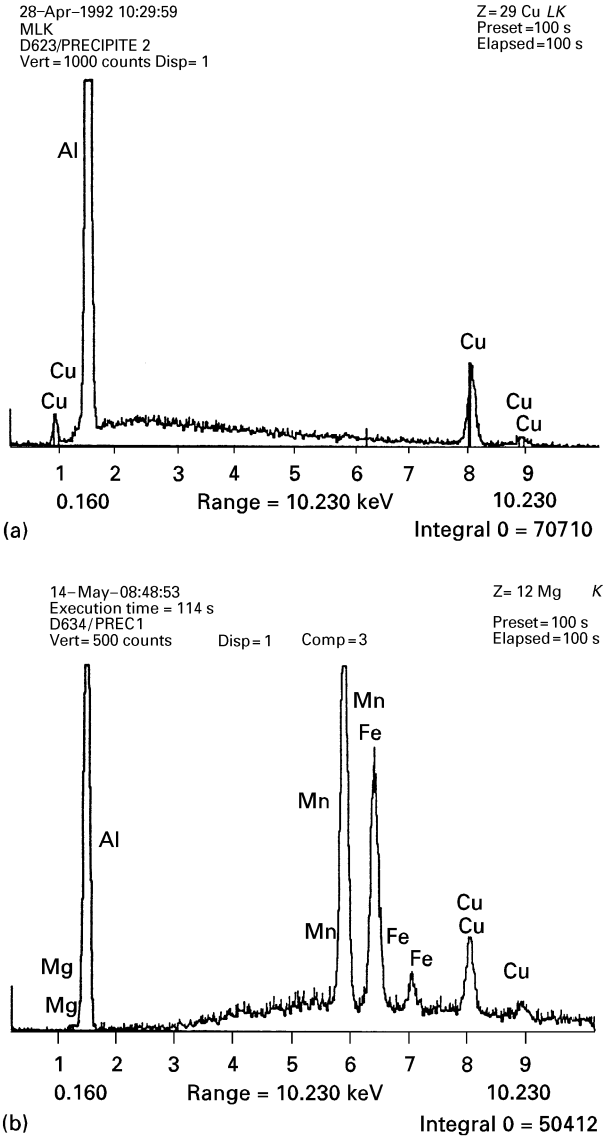

Figure 13 X-ray spectra of the precipitates observed on the fractured surfaces shown in Figs 10b and 11b.

obvious adhesive failure zones, in the presence of smooth patches characteristic of a brittle junction, are observed. In addition, some initial mechanical polishing features are still visible on the failure surface. In the latter case (Fig. 12b), the fractured surface is completely ductile. The mechanical polishing striations have disappeared and many precipitates are observed. It seems that the ductile failure of the welded joint, and thus its mechanical properties enhancement (see also Figs 7 and 8), is associated with the presence of precipitates at the origin of dimples formation. In fact, the plastic deformation around the precipitates forms many elongated dimples in the tensile strain direction, followed by a pulling out of the parent metal.

The SEM observations of the fractured surfaces of the welded specimens at 550 and 575 °C, show two kinds of precipitate of different compositions. The first are of an oblong shape, the second are rounded. The X-ray spectra of the oblong precipitates revealed a high copper concentration, which might concern the Al_2Cu precipitates (Fig. 13a). The second, precipitates located inside the dimples cavities, revealed a high concentration of manganese, iron and a small presence of magnesium and copper (Fig. 13b). Thus, the mechanical properties enhancement of the welded joints is associated with chemical modifications of the two surfaces to be welded, during the heating cycle.

4. Discussion

From the above results, it appears that the welded joint strength reaches the treated base material values for welding temperatures above 525 °C, and it is definitely weaker below this temperature. According to the ternary phase diagram of the Al–Cu–Mg system, this temperature corresponds to the solidus temperature boundary of the A 2017 alloy [2–4]. In other words, the presence of a small amount of liquid phase enhances the welded joint strength. This performance is also related to the diffusion welding processes efficiency at high welding temperatures.

In fact, in spite of the strong structural modifications of the base metal, the optimum welding parameters are precisely obtained for a welding temperature of 575 °C, a welding time of 2 h and a welding pressure of 2 MPa. According to the failure strain or the failure energy, it appears that the welded joints behaviour is substantially lower than that of the treated sample, even if the strengths are in the same range of magnitude. The differences between the behaviour of the welded and the treated samples are in creased by the

dynamic loading test, and thus the embrittlement of the interface zone is made more obvious by loading the samples at high strain rates. An increase in the welding pressure from 2 MPa to 5 MPa for 30 min, enhances slightly the joint strength, in spite of the high welding deformations. Consequently, an increase in the welding pressure above 2 MPa must be avoided.

The SEM observations showed that at low welding temperature (500 °C), the failure surface is brittle, the polishing striations remain visible and dimple-free, whatever the welding parameters. In contrast, at high welding temperature (575 °C), the fractured surfaces show a ductile failure aspect in the presence of dimples and precipitates, while the polishing features have disappeared. Such a morphology difference explains the dependence of the aspect of the failure surfaces on the welding parameters. Although the welded joint strength reaches that of the treated material, it is observed that failure often occurs in the interfacial zone. This shows that, even at 575 °C, the weaker part of the welded sample is always the joint area, because of its embrittlement, despite some observations of the pulling out of parent metal.

The precipitates present in the welded joint interface, are lengthened in the tensile strain direction by the tensile elongation. Consequently, the welded joint strength might be increased by the mechanical anchoring of the two welded surfaces. The X-ray spectra show that these precipitates, of different shapes, contain the base material chemical components. First, the oblong shaped precipitates might be the Al_2Cu precipitates, while those of rounded shape, located inside the dimple cavities, contain magnesium, copper and high concentrations of manganese and iron.

5. Conclusion

This work reports the study of the mechanical properties of diffusion-welded joints under high-rate tensile loading. The dynamic tests, carried out on a Hopkinson bar linear assembly, yielded definite information on the joint efficiency, revealing detailed differences in the mechanical properties, which were not clearly visible in the earlier dynamic loading test. The influence of the main welding parameters has been studied, the precise trends of which have been confirmed. However, the spread in the measurements was large at lower welding temperatures, but small at higher temperatures. In the former case, this is due to the brittle nature of the welded sample failure, according to SEM observations of the fractured surfaces.

The SEM observations and the X-ray analysis show that at lower welding temperature the fractured surfaces are brittle, precipitate- and dimple-free. Above 525 °C, the joint strength is enhanced and reaches the treated base material values. In contrast, failure elongation of the welded joints remains very weak and clearly lower than the treated samples, whatever the welding temperature. An increase of the welding time from 30 min to 2 h substantially enhances the welded joint strength. It has also been established that an increase in the welding pressure from 2 MPa to 5 MPa slightly enhanced the welded joint mechanical properties. The increasing rate of the failure energy, as a function of the welding temperature, is smaller than that of the failure strength, because of the brittleness of the welded joints.

In static tests [2, 3] it appeared that above 525 °C, the tensile strength of the diffusion-welded joints was practically independent of the other welding parameters (time, pressure, surface state). In contrast, in dynamic tests, the mechanical properties of the welded joints depend significantly on the welding parameters (time, pressure and temperature). Thus, an increase in the welding temperature enhances the welded joint strength, and welding temperatures above 525 °C are needed, for joint strengths to reach values close to those of the treated material. However, the solidus temperature of A 2017 is close to 525 °C, and above this temperature, a small amount of liquid phase coexists with the solid phase on the sample surface, facilitating the bonding of the pieces to be welded. Consequently, the presence of precipitates, in the welded interface, leads to dimple formation, thus improving the mechanical properties of the welded joint, by the mechanical anchoring of the two welded surfaces. Hence, it is concluded that high-rate tensile tests can be a very discriminating technique to determine the diffusion welded joints efficiency, and to help in the best choice of operating conditions.

Acknowledgements

This work was partly supported by the "chocs et Développements" laboratory team at Ecole Centrale de Nantes, (France). The authors thank Dr M. Dannawi for the dynamic tensile loading tests and the discussions participations.

References

1. M. CAILLER, O. DEBBOUZ, M. DANNAWI and T. LATOUCHE, *J. Mater. Sci.* **26** (1991).
2. T. LATOUCHE, M. CAILLER and S. K. MARYA, Effect of some process parameters on the diffusion welding of 2017 Al alloy: in Proceedings of the "4th International conference on aluminium weldements (INALCO, 88), Tokyo, Japan (April, 1988) pp. 21–37.
3. *Idem*, Soudage et Techniques connexes, No. 1–2; in "Proceedings, 4ème Journée du soudage (JN4)", (Société Française de Métallurgie, Paris, 1989) pp. 54–65.
4. T. ENJO, K. IKEUCHI, M. ANDO and K. HAMADA, *Trans. JWRI* **14** (2) (1985) 93.

Received 8 December 1995
and accepted 2 July 1996